ANL/PHY/CP-99800

ATLAS 10 GHz ECR Ion Source Upgrade Project

D. P. Moehs, R. Vondrasek and R. C. Pardo

Argonne National Laboratory, Physics Division, 9700 S. Cass Ave., Argonne IL 60439, USA: E-mail: moehs@anlphy.phy.anl.gov

D. Xie

Berkeley Ion Equipment Inc., 3400 De La Cruz Blvd. V, Santa Clara CA 95054, USA

RECEIVED
OCT 12 1999
OSTI

A major upgrade of the first ATLAS 10 GHz ECR ion source, which began operations in 1987, is in the planning and procurement phase. The new design will convert the old two-stage source into a single-stage source with an electron donor disk and high gradient magnetic field that preserves radial access for solid material feeds and pumping of the plasma chamber. The new magnetic field profile allows for the possibility of a second ECR zone at a frequency of 14 GHz. An open hexapole configuration, using a high energy-product Nd-Fe-B magnet material, having an inner diameter of 8.8 cm and pole gaps of 2.4 cm has been adopted. Models indicate that the field strengths at the chamber wall, 4 cm in radius, will be 9.3 kG along the magnet poles and 5.6 kG along the pole gaps. The individual magnet bars will be housed in austenitic stainless steel allowing the magnet housing within the aluminum plasma chamber to be used as a water channel for direct cooling of the magnets. Eight solenoid coils from the existing ECR will be enclosed in an iron yoke to produce the axial mirror. Based on a current of 500 A, the final model predicts a minimum B field of 3 kG with injection and extraction mirror ratios of 4.4 and 2.9 respectively.

DISCLAIMER

DISCLAIMER

1. INTRODUCTION

The ATLAS facility at Argonne National Laboratory provides beams of heavy-ions at energies of up to 17 MeV/A for research in nuclear and atomic physics[1]. Beams of any element are potentially available. In a typical year, beams from nearly 30 different isotopic species are provided from protons to uranium. The majority of these beams have been produced by the ATLAS ECR-I[2] ion source from solid materials.

ECR-I has operated reliably since 1987 and has provided over 30,000 hours of beam for ATLAS. The source dates from the 'first generation' period of high charge state ECR ion sources, utilizing a two-stage design and a radio frequency (RF) of 10 GHz. As the only ECR ion source for ATLAS, time for development and source improvements was greatly constrained. Now with the completion of a new, second, ECR ion source[3] for ATLAS it is possible to undertake a significant redesign of the ECR-I source and incorporate many of the new techniques and concepts developed over the past ten years[4] in a newly designed incarnation of ECR-I.

The primary goal for upgrading the ECR-I ion source is to significantly improve the average charge state distribution produced by the source, typically shifting the average charge state up by approximately 10%. A second goal is to increase the total useful beam current extracted by up to a factor of two. These goals are to be achieved while maintaining a source design that continues to emphasize the importance of solid feed material. The major features of the new source are:

1. 10 GHz RF operation will be continued, but the magnetic field design will support operation at 14 GHz.

2. Large radial access ports into the plasma region will be maintained in conjunction with a strong hexapole field that keeps the ECR resonance zone well confined.

3. A single stage source design with an on-axis electron donor disk replacing the function of the old first stage.

4. Use of an aluminum plasma chamber to make maximum use of the high secondary electron yield of aluminum oxide surfaces.

5. The control system of the new source will be fully incorporated into the main ATLAS VISTA control system.

II. SOURCE DESIGN

The basic structure of this source is shown in Fig. 1. Both the injection and extraction tanks are shown along with the iron yoke surrounding the solenoid coils. The plasma chamber is 30 cm long from the bias disk to the extraction aperture and 8 cm in diameter. The 10 GHz RF line and all of the gas feeds are coupled into the source through the injection tank on the left.

Both the injection and extraction coils will be mounted from a common base plate. While the extraction coil and plasma chamber will be permanently fixed in position, the injection coil will sit atop a rail system allowing the coil, iron yoke and injection tank to be rolled back from the plasma chamber roughly 1.2 m. To achieve the greatest flexibility the inner iron on both the injection and extraction coils will be partially removable providing a maximum working gap of 10.7 cm between the coils.

An open hexapole configuration with 6 radial ports 2.8 cm long and 1.7 cm wide through the plasma chamber allows access to the plasma for solid material feeds, pumping of the source region and plasma diagnostic studies. Pumping of the plasma chamber will be provided through two of the radial ports at an estimated rate of 40 l/s. Figure 2 shows a magnified view of the plasma chamber highlighting the radial ports, hexapole arrangement and water cooling channels at the base of each magnet block. The plasma chamber will be constructed out of 1061 aluminum and have an inner diameter of 8 cm. The inner and outer corners of the magnet blocks are at radii of 4.5 cm and 10.5 cm respectively. The easy axis angles are at 38 degrees relative to the center of each pair of magnet blocks. The hexapole magnet bars will be encased in austenitic stainless steel and then housed in channels within the plasma chamber walls. These same channels will be used for direct water cooling of the hexapole.

Neglecting water flow around the magnet bars the effective water-channel cross section is 0.38 cm^3. A physical model of this region of the plasma chamber 30.5 cm long was constructed to determine if sufficient cooling to the hexapole is provided. Test data at 1 gal/min and a pressure near 80 psi, with an estimated energy flux of 130 watts, produced a 1° C increase in the water temperature and a 10 to 12° C increase in the external aluminum. Based on a series of these measurements at different flow rates and different external temperatures, the hexapole should remain within a few degrees of the water temperature, even under a 2 kW load. To insure sufficient water flow at the available pressure, three parallel water leads will be installed.

III. MAGNET DESIGN

Eight of the original solenoid coils will be reused to produce the axial mirror. The solenoid field including the surrounding iron yoke was simulated using the POISSON[5] code and the iron was adjusted to produce the best B field gradients. The dashed line in Fig. 3 shows the resulting axial field for a current of 500 A in both coils. The minimum-B field between the two coils is 3.0 kG while the injection and extraction mirror ratios (MR) are 4.4 and 2.9 respectively. Additional simulations indicate that the MR go up as the current is reduced. For example, at the minimum current of 350 A, which insures that there is no 10 GHz on axis resonance zone in the near extraction region, a minimum-B field of 2.2 kG is produced with MR of 4.8 and 3.0. When a second frequency at 14 GHz is added the minimum current required is 425 A, producing a minimum-B field of 2.9 kG and MR of 4.5 and 2.9. Thus in the case where a lower B-field gradient is desired, which might be the case for producing low charge states, some of the iron around the coils should be removed (see Source Design above). Based on the model, the position of the extraction gap has been placed at the peak of the extraction B field, which minimizes its effects on the plasma.

In order to achieve a large radial B-field gradient and wide radial ports, an open hexapole configuration using a high energy-product Nd-Fe-B magnet material was selected. Computer models of this configuration were produced separately using PERMAG[6] and PANDIRA[5]. The main distinction between these two codes is that PERMAG is capable of generating 3D fields but does not consider the possibility of demagnetization while PANDIRA includes the coercive force (H_c), accounting for demagnetization effects, but only supplies a 2D-field profile that ignores end effects. With these limitations in mind, an initial 2D model of the hexapole was generated using PANDIRA in order to optimized B_r and B_ϕ (field profile in Ref. 7). Once the fields were optimized a second model using PERMAG was generated and the results were found to be identical to the PANDIRA model. Assuming demagnetization is not a factor for the high H_c material selected, PERGMAG was subsequently used to generate a 3D-field profile so that end effects could be investigated. Without considering the effects of the iron on the hexapole field, a zero order approximation was generated by combining both the solenoid and hexapole field profiles via superposition. The three lines of interest in this model lie along the two magnet poles and along the center of the pole gap. In all three cases, cancellation effects on the extraction side were minimal and well handled by shaping the iron plug forming part of the extraction region. However, cancellations on the injection side, associated with magnet bars with their magnetization direction pointing away from the center of the hexapole, were hardest to deal with because of the very strong solenoidal field in that region. The B field as a function of the axial position (z) for three different radial values (r) is plotted in Fig. 3. Ideally the radial field lines should not cross spatially as they do near z = 20 cm. In this case, simple shaping of the iron yoke did not modify the field profile significantly. The only thing that made a significant difference was the reduction of the solenoid current but this compromises the peak B field, which was deemed more important. The field crossing seen near Z = 50 cm corresponds to an off axis point just outside of the extraction aperture. At 14 GHz a resonance zone will appear in this region with very weak confinement. This effect has been observed in ECR-II, which has a similar iron extraction yoke configuration, but the effect on the extracted ions has not yet been determined.

IV. CURRENT PROJECT STATUS

Table 1 presents a summary of the ECRIS parameters that have been discussed. Additional modeling of the extraction region, including electric and magnetic fields as well as space charge effects, is being carried out using PBGUN[8]. The puller location and configuration as well as the effects of the electrostatic focusing lens, just outside the source, are being studied.

Conversion to the ATLAS master control system is underway but since ECR-I remains in operation this transition has been limited in scope. At present the gas manifold has been successfully interfaced through CAMAC and fiber optic links. Further updates in the control system will take place as scheduling permits.

The hexapole magnets have been ordered and the plasma chamber and iron yoke assembles will be submitted for fabrication in the near future. The decommissioning of the existing 10 GHz ECR is planned for late Fall 1999 with initial testing of the new ECRIS in early 2000.

The U.S. Department of Energy Nuclear Physics Division, under contract W-31-109-ENG-38 supported this work.

---

[1] L. M. Bollinger, R. C. Pardo, K. W. Shepard, J. M. Bogaty, B. E. Clifft, F. H. Munson , and G. Zinkann, Nucl. Instrum. Methods Phys. Res. A **328**, 221 (1993).

[2] R. Pardo, Nucl. Instrum. Methods Phys. Res. B **40/41**, 1014 (1989).

[3] M. Schlapp, R. C. Vondrasek, J. Szczech, P. J. Billquist, Z. Q. Xie, C. M. Lyneis, R. Harkewicz and R. C. Pardo, 13th Int. Workshop on ECR Ion Sources, College Station TX, 22 (1997).

[4] D. P. May, Rev. Scien. Instrum. **69**, 620 (1998).

[5] J. H. Billen and L. M. Young, Los Alamos National Laboratory report LA-UR-96-1834 (revised 1998).

[6] Z. Q. Xie and T. A. Antaya, National Superconducting Cyclotron Laboratory, Michigan State Univ., E. Lansing, PERMAG manual, provided by Z. Q. Xie.

[7] D. P. Moehs, R. Vondrasek, R. C. Pardo and D. Xie, 14th Int. Workshop on ECR Ion Sources, Geneva, Switzerland (1999).

[8] J. E. Boers, ICOPS Conf. Proc., Dallas TX, 1995.

FIG. 1. Schematic of the new single-stage 10 GHz ECRIS with the injection tank on the left. Pumping of the plasma chamber will be provided through two of radial ports and through the extraction region.

FIG. 2. An exploded view of the plasma chamber highlighting the hexapole magnets within their housing, the water channels and the easy axis angle relative to the common surface of each magnet block pair. The arrows indicate the magnetization direction.

FIG 3. A slice from the 3D magnetic field model showing the spatial overlap of the B field resulting from hexapole end effects. Z = 0 corresponds roughly to the outer edge of the injection yoke. The coil current was 500 A.

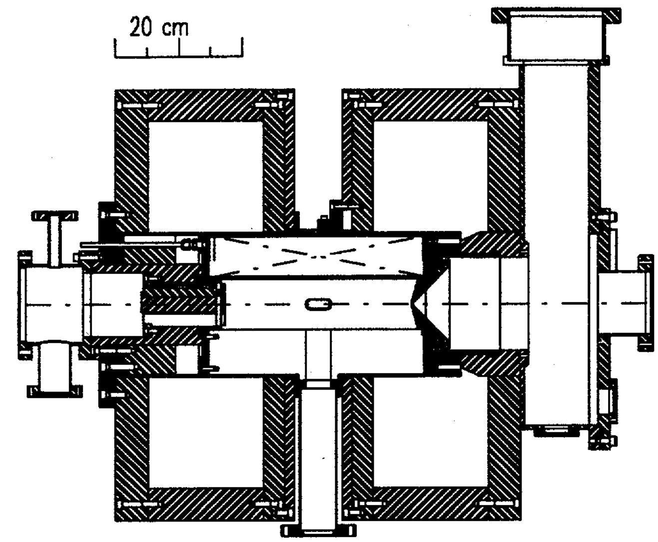

Fig 1

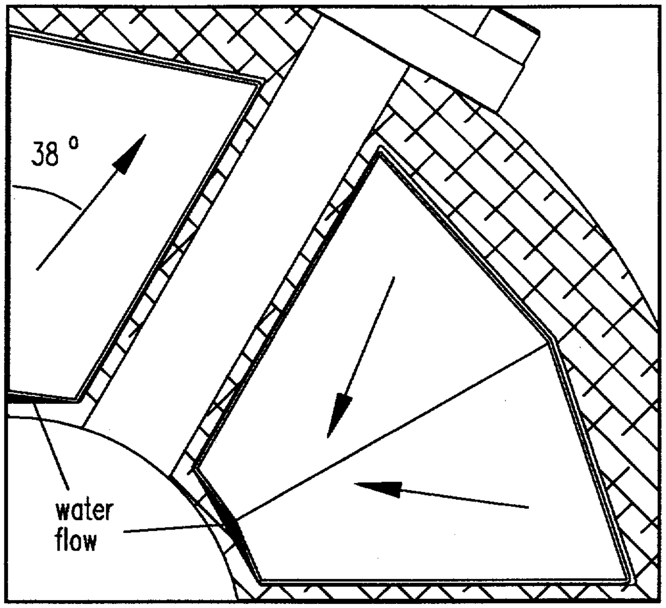

Fig 2

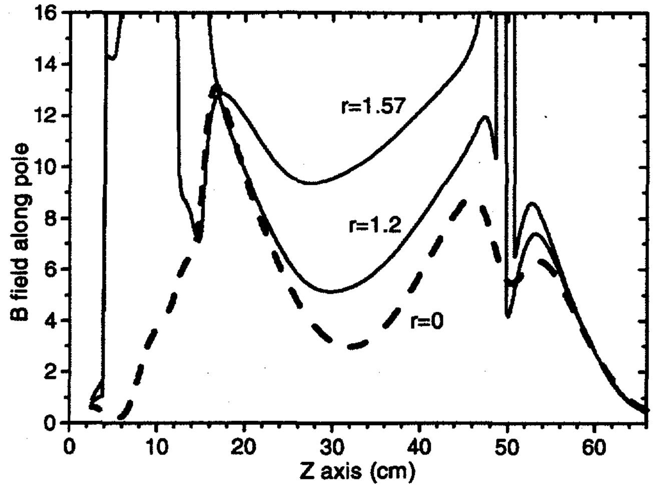
r=1.57
r=1.2
r=0
B field along pole
Z axis (cm)
0
2
4
6
8
10
12
14
16
0
10
20
30
40
50
60

Fig 3

Table I: Summary of ECRIS parameters

Microwave Frequency	10 GHz
	14 GHz possible
Aluminum plasma chamber	
Diameter	8.0 cm
Radial ports	2.8 cm by 1.7 cm
Water channel cross section	0.38 cm^2
Solenoid coils	
Current range for 10 GHz	350 – 500 A
Minimum Field (500 A)	3.0 kG
Injection side MR	4.4
Extraction side MR	2.9
Hexapole	
Length	33.0 cm
Easy axis angle (radial ref.)	38.0°
B_r Pole tip field, r = 4 cm	≈ 9.2 kG
B_Φ Gap field, r = 4 cm	≈5.6 kG
Cooling water	
Input temperature	≈ 11° C
Head pressure	80 psi
Max. expected $\Delta T_{hexapole}$	< 10° C at 1.0 gpm
For a 2 kW input	per channel
Max. expected ΔT_{coils}	< 30° C at 4.0 gpm
For a current of 500 A	per coil